ISSN 1062-8738, Bulletin of the Russian Academy of Sciences: Physics, 2024. © Pleiades Publishing, Ltd., 2024.

IR-Thermometry-Based Thermal Balance Model for Blood Flow Rate Express-Analysis

M. E. Stepanov[a, b, *], A. A. Vlasov[a, b], M. Yu. Suchkov[b], K. R. Karimullin[c], A. V. Naumov[b, c], I. I. Eremin[a], B. A. Akselrod[a], and E. V. Khaydukov[a, b, d, e]

[a] *Petrovsky National Research Centre of Surgery, Moscow, 119991 Russia*

[b] *Moscow State Pedagogical University, Moscow, 119435 Russia*

[c] *Lebedev Physical Institute, Russian Academy of Sciences, Moscow, 119017 Russia*

[d] *Shemyakin and Ovchinnikov Institute of Bioorganic Chemistry, Russian Academy of Sciences, Moscow, 117997 Russia*

[e] *Mendeleev University of Chemical Technology of Russia, Moscow, 125047 Russia*

*****e-mail: Stepanov_me@mail.ru*

Received October 8, 2024; revised October 22, 2024; accepted November 6, 2024

Abstract—Infrared (IR) thermometry is a modern high-resolution method of remote temperature distribution monitoring on any open surface. The non-invasive method of IR thermometry is successfully used to solve several biomedical problems, since the temperature distribution on the human body contains physiological state information of diagnostic importance. We show that this information is not only diagnostically valuable but can also serve as a predictor of future complications. In the field of intraoperative observations IR thermometry allows one to assess circulatory disorders and take preventive measures timely. Obviously, this direction requires the development of express thermal analysis methods that can be implemented in real time by considering only basic significant patterns excluding necessity of time-consuming numerical modeling. In this paper, using the example of an occlusion test, as well as cooling and heating tests on a finger of healthy subjects, a simple model of thermal balance is considered, which allows one to quantitatively estimate the relative blood flow rate.

Keywords: biomedicine, IR thermometry, IR thermography, thermal image analysis, blood flow, blood circulation, occlusion test, dynamic cooling, dynamic warming, heat transfer in living tissues

DOI: 10.1134/S1062873824709413

INTRODUCTION

Like all endotherms, humans maintain body temperature within evolution-set limits, optimal for complex biochemical processes [1]. According to Planck's law the scale of this thermal energy for normal body temperatures falls on the middle and far infrared range of the spectrum (~4–100 μm), accessible for high-resolution observation using modern microbolometers and quantum detectors. An example of a thermal image (thermography) obtained using a Xenics Gobi-384 IR camera can be seen in Fig. 1, where the face of one of the authors is photographed in a cold room.

Methods of optical fluorescence thermometry have been actively developed recently, including the search for and study of new luminescent materials [2–5].

Due to the development of modern microbolometers and quantum detectors, the IR thermometry method is used in the diagnosis of several socially significant diseases [6]. Thus, according to [7], the probability of aggressive breast cancer in women reaches 12.3% preponderated in frequency of occurrence only by lung cancer. The standard diagnostic approach in detecting the tumor is mammography, which is an X-ray image of the breast, but this method is reliable only for older ages (from 50 years), since the tumor is poorly distinguishable against the background of dense tissue, while the average density of breast tissue decreases with age. IR thermography is gradually becoming a complementary diagnostic tool, since it has no side effects while still allowing diagnosing a tumor. The IR camera records the abnormal temperature distribution on the skin occurring due to the irregular vascular network formed in the tumor tissue, as well as the accumulated molecular agents (nitric oxide) increasing local blood flow and, as a result, leading to impaired heat exchange in the tumor area. At the same time, clinical studies show (see [7] and references therein) that an increased density of breast vessels, which can be observed using IR methods, serves as a risk factor of tumor occurrence in the next 2–4 years, i.e. the method can be used to take preventive measures, which can significantly improve the prognosis.

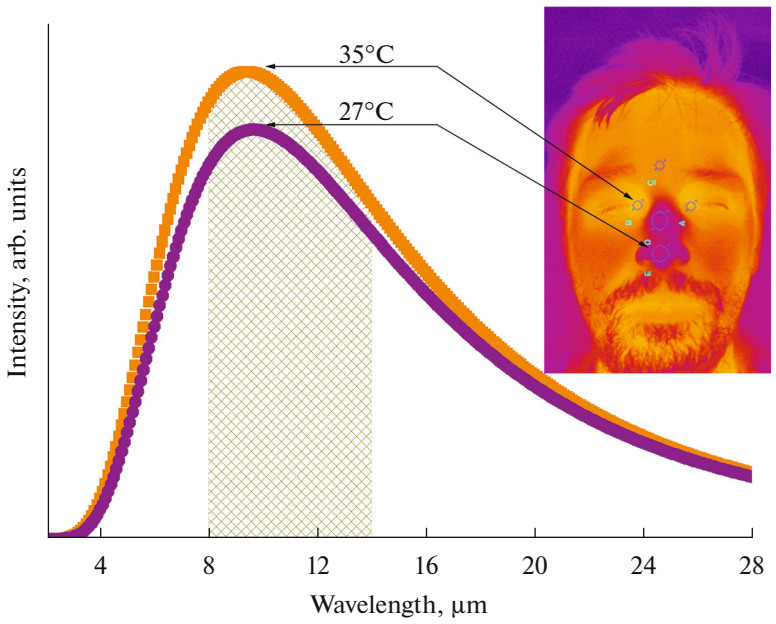

Fig. 1. Planck blackbody radiation curves for temperatures 27 and 35°C, corresponding to the areas of the nose and eyes in the thermal image of a face recorded in cold-room conditions. The number of photons in each case is determined by the temperature and is proportional to the area under the curve in 8–14 μm region recorded by the IR camera (shown by hatching). It allows temperature to be calculated based on the integral brightness of each pixel. The color scale is assigned arbitrarily.

A similar approach can be applied to the diagnosis of skin cancers, where the standard approach is based on subjective assessment during an external examination followed by a biopsy to confirm the diagnosis. In [8], it is shown that dynamic IR thermometry (when temperature returns to normal after cooling is analyzed) can distinguish malignant tissue from healthy one with high reliability.

The IR thermometry method is also applicable to the problem of assessing the degree of skin burn damage. The authors [9] proposed a quantitative IR thermographic method, which allows making a prognosis of spontaneous wound healing probability in the three-week period following skin burn, which is critical for deciding of skin graft transplantation. Since heat transfer in damaged tissues is impaired depending on the severity of the burn, assessing heat transfer in damaged tissues has significantly reduced the number of transplantations and their costs while increasing the effectiveness of therapy since skin graft survival can be also monitored by this method [10].

Another important IR thermometry application is detection of tissue innervation disorders. Since thermoregulation at the level of body regions is controlled by the central nervous system, deviations in their temperature may indicate disorders in the transmission of nerve signals. For example, in type 2 diabetes (affects more than 6% of the world's population [11]) a complication called diabetic foot can occur. As clinical research data show (see review [6] and references therein), timely analysis of thermographic data allows one to identify the development of inflammation in the foot and begin therapy in time, reducing the risk of future complications tenfold.

IR thermometry is used to diagnose cardiovascular diseases, which remain the most significant health problem worldwide [12]. Since blood flow is the main channel for heat transfer within the body, its disturbances can often be detected during thermographic studies. A demonstrative example is heart failure caused by blockage of coronary vessels. IR thermography in coronary artery bypass grafting has several applications—from specifying the position of coronary vessels (including the blocked area) under the layer of fatty tissue that often surrounds the heart, to checking the success of the operation by the presence of warming of the implanted vessel by the blood flow [13].

Measuring local temperature is important for assessing changes in the degree of oxygenation, for example, during photodynamic effects on biological tissues [14], since stimulation of blood microcirculation during low-intensity light irradiation is most likely due to thermal mechanisms of utilization of absorbed energy.

Finally, recent research provides an increasing amount of evidence that monitoring of blood flow microcirculation may be of no less importance than macrocirculation and, moreover, they may be independent of each other [15–18]. Disturbances in blood flow microcirculation can lead to parenchymal cell damage and death, which disrupts the functioning of body tissues and may lead to serious consequences.

For example, during cardiac surgery, future complications may not correlate with systemic blood flow parameters (minute blood volume, arterial pressure, etc.), which are usually maintained within optimal limits. Instead, complications may be associated with disturbances in tissue microcirculation (capillary network density, network homogeneity, speed and nature of red blood cell movement, etc.), which are usually not monitored due to the lack of suitable methods [19].

Deviation of microcirculation parameters can become an extremely important marker for taking measures to prevent postoperative complications. The question of the possibility of measuring microcirculatory parameters in situ during surgery using IR thermometry has not been fully studied and is of great scientific and practical interest [20]. Of course, the most significant measures to correct circulatory impairments can only be taken intraoperatively, when the problem can be fixed before its development. Such specificity is compatible only with express methods of diagnosing disorders, which limits the possible range of analysis tools, excluding detailed mathematical models that require numerical modeling. This raises the question of developing the simplest and easily-to-interpret models compatible with real-time monitoring constraints.

IR-THERMOMETRY-BASED THERMAL BALANCE MODEL FOR BLOOD FLOW RATE ASSESSMENT

Here we discuss in detail one of the possible thermal models. Since the basic information provided by the IR thermography method is the temperature distribution on the surface under study, it is important to understand what influences the process of its establishment. Consider a special case of small, dry, uncovered area of human skin at room temperature. This area is warmed from the inside by the heat of underlying tissues and cooled from the outside by the cold room air. The resulting skin temperature $T_s(t)$ measured by the IR detector. This temperature depends on time t until the process reaches equilibrium. For simplicity, we will use a single-layer model when the temperature inside and outside the body are uniform. The heat balance equation for this area:

$$W_\mathrm{i} - W_\mathrm{e} = cm\frac{\Delta T_\mathrm{s}}{\Delta t}. \tag{1}$$

Here $W_i = \dfrac{\Delta Q_i}{\Delta t}$ [W] is the internal heat exchange rate; $W_e = \left|\dfrac{\Delta Q_e}{\Delta t}\right|$ [W] is theexternal heat exchange rate; c [J/°C kg] is the skin heat capacity; m [kg] is the skin mass; ΔT_s [°C] is the temperature change during the time step Δt.

It is rewarding to adopt a simplifying linear approximation, in which the heat exchange rates are proportional to temperature differences on different sides of the surface:

$$W_\mathrm{i} = h_\mathrm{i}A\left(T_\mathrm{i} - T_\mathrm{s}\left(t\right)\right), \tag{2}$$

$$W_\mathrm{e} = h_\mathrm{e}A(T_\mathrm{s}(t) - T_\mathrm{e}). \tag{3}$$

Here A [m^2] is the skin area; h_i and h_e [W/°C m^2] are the thermal or heat conductance coefficients that determine the rate of heat exchange between the surface and the tissues and the room, respectively [21]. Thus, within the framework of this model, we assume that the rate of heat exchange depends on the temperature differences scaled by h_i and h_e times. The coefficient h_i is determined by the blood flow rate, thermal conductivity of the tissues and tissue metabolism (for example, muscle metabolism) in the measured area. The coefficient h_e is determined by air convection and humidity, the presence of hair or other external thermal insulation. We call ratio $h_\mathrm{i}/h_\mathrm{e}$ of the coefficients the blood flow index.

Since we consider small area of skin, it can be approximated to be flat. Then its mass is $m = \rho V = \rho AL$ (proportional to the area A, thickness L and mass density ρ). If we put everything together and substitute back in the original heat balance equation, we get:

$$h_\mathrm{i}T_\mathrm{i} + h_\mathrm{e}T_\mathrm{e} - \left(h_\mathrm{i} + h_\mathrm{e}\right)T_\mathrm{s}\left(t\right) = c\rho L\frac{\Delta T_\mathrm{s}\left(t\right)}{\Delta t}. \tag{4}$$

The main advantage of the model is that the resulting equation can be solved analytically. If we assume that h_i and h_e are constant, the solution takes the form:

$$T_\mathrm{s}\left(t\right) = \left(T_{\mathrm{s},0} - T_\mathrm{static}\right)e^{-\frac{\left(h_\mathrm{i}+h_\mathrm{e}\right)\left(t-t_0\right)}{c\rho L}} + T_\mathrm{static}. \tag{5}$$

Where $T_{\mathrm{s},0}$ [°C] is the initial temperature at $t = t_0$; T_static [°C] is the stationary temperature, corresponding to $t \to \infty$, when exponential part vanishes. Analytical expression for T_static is of importance for the subsequent analysis:

$$T_\mathrm{static} = \frac{h_\mathrm{i}T_\mathrm{i} + h_\mathrm{e}T_\mathrm{e}}{h_\mathrm{i} + h_\mathrm{e}}. \tag{6}$$

From (6) it is clear that the values of the thermal coefficients h_i and h_e determine the proportion in which the equilibrium temperature will be "fixed" in relation to the external T_e and internal T_i (for example, $T_\mathrm{static} \to T_\mathrm{e}$ at $h_\mathrm{e} \gg h_\mathrm{i}$ and vice versa). In the general case of non-zero and non-infinite h_i and h_e, the skin temperature will be a weighted average between T_e and T_i with weights $\dfrac{h_\mathrm{e}}{h_\mathrm{i} + h_\mathrm{e}}$ and $\dfrac{h_\mathrm{i}}{h_\mathrm{i} + h_\mathrm{e}}$. For us, this means the possibility of estimating the relative values of $h_\mathrm{i}/h_\mathrm{e}$ in the stationary (static) case, when we can assume

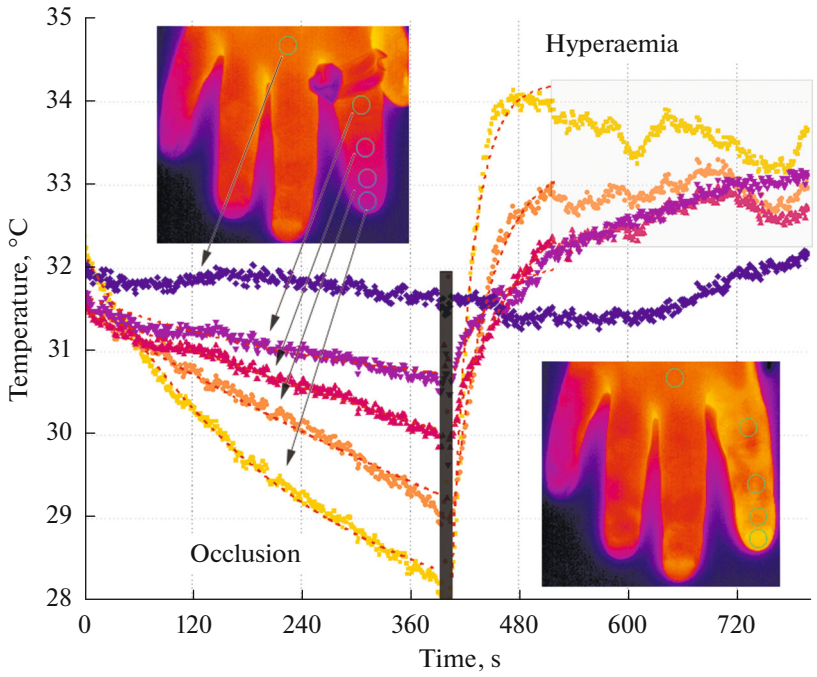

Fig. 2. Temperature changes in different areas of the index finger skin during occlusion (Occlusion, thermal image in the lower-right corner) and after occlusion (Hyperaemia, image in the upper-left corner). The areas of the finger where the temperature is measured are highlighted with cyan circles in the inserts: nail (yellow graph), distal (orange), intermediate (pink) and proximal (lilac) phalanges, as well as the back of the hand (purple). Red dotted curves are approximations obtained using the developed model. The gray frame on the right side highlights the area of highly nonlinear blood flow. The area corresponding to the moment of occlusion removal is hatched black. Color scale 24.5–36.5°C.

thermal equilibrium, since the ratio h_i/h_e can be expressed directly from Eq. (6):

$$h_i/h_e = \frac{T_{static} - T_e}{T_i - T_{static}}. \quad (7)$$

EXPERIMENTAL BLOOD FLOW EVALUATION

We will evaluate the applicability of the model in the case of finger occlusion, cooling and heating experiments, where we'll use it to determine the index h_i/h_e (proportional to the blood flow in the area under study). The results of the occlusion test are shown on Fig. 2.

Several observations can be made from the graphs in Fig. 2. First, under normal conditions (without occlusion), the temperature of the back of the hand fluctuates with an amplitude of ~1°C. The temperatures of the fingers behave similarly. This is due to the normal regulation of blood flow at the level of the central nervous system. Second, after obstruction of the vessel's temperature starts to decrease due to the lack of blood flow, gradually approaching room temperature (24.4°C) because in the heat balance Eq. (4), the heating associated with the blood flow is now minimized. In addition, the thinner and further away parts of the fingers (nail and distal phalanx) cool faster due to more effective air cooling and less mass (high area-to-volume ratio). Third, after occlusion the blood flow begins to heat the finger rapidly to temperatures that can be even higher than the initial ones (hyperemia). The increased blood flow is associated with the work of the local regulatory mechanism of increasing blood flow through the dilation of the vascular lumen (vasodilation) in response to metabolites accumulated during occlusion. Fourth, if thermal diffusion were the main mechanism of heat exchange, warming would occur from the warmer knuckles towards the fingertip, but we see the opposite picture: the most rapid growth is observed in the nail area, which is associated with a significant number of microcapillaries in this area. Fifth, as can be seen in the thermal image of the index finger in the upper left corner of Fig. 2 (corresponds to 470 s on $T_s(t)$ graph), the spatial pattern of hyperaemia (return of blood flow) is quite complex and heterogeneous: the areas closest to the large vessels of the finger warm up first, then, due to diffusion and microcirculation, the intermediate areas filled with smaller vessels gradually warm up.

Heat balance model applied to heat exchange processes allows obtaining a pattern of changes in blood flow, shown in Fig. 3. Here, the values corresponding to the normal (orange columns) are obtained within the framework of the static picture calculated using Eq. (7), while the dynamics of cooling during occlu-

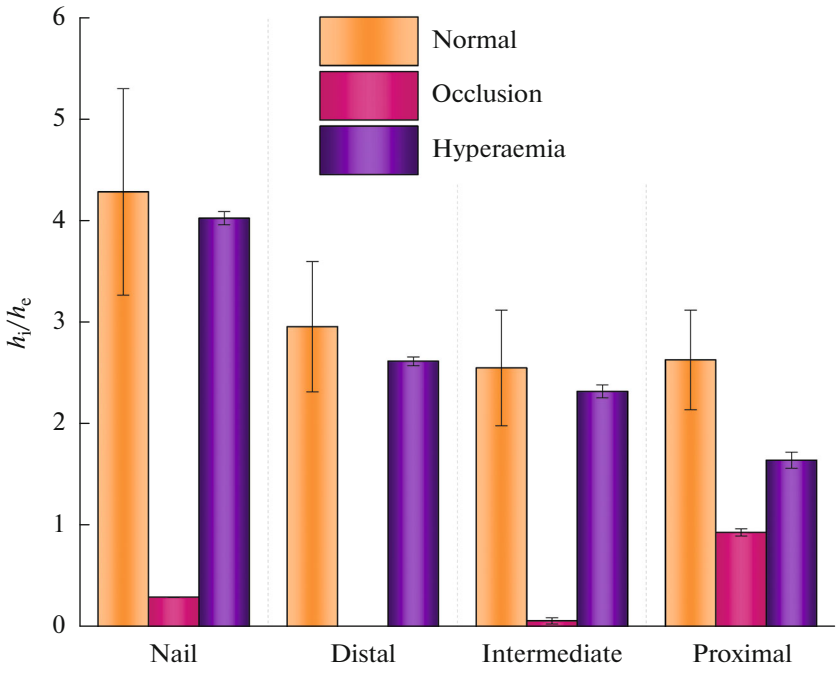

Fig. 3. The ratio of thermal coefficients h_i/h_e for different areas on the index finger (Nail, Distal, Intermediate, Proximal) in the static normal state before occlusion (orange); during occlusion (pink); after occlusion during hyperemia (lilac).

sion (pink columns) and the dynamics of reheating during hyperemia (lilac columns) correspond to the dynamic approximations (5), shown by the red dotted lines in Fig. 2.

As follows from the data, occlusion significantly reduces blood flow, which is consistent with the sharp drop in h_i/h_e (see Fig. 3). After removal of the clamp, blood flow is restored to levels that (considering the temperature fluctuations, measures during 10-min observation under normal conditions, see the purple graph in Fig. 2) may be higher than the initial ones (reactive hyperemia). Thus, the presented simple model of heat balance allows us to obtain useful indirect estimates of the blood flow in both static and dynamic cases and compare them with each other.

Now let us apply the heat balance model to assess blood flow during dynamic stress tests of cooling/heating of local hand areas. Figure 4 shows temperatures corresponding to warming up of different areas of the index finger after cooling in cold water at 20°C for 90 s. Consider the nail temperature graph in some detail: its course is quite complex, demonstrating a set of sharp bends due to blood flow instability. Moreover, its dynamics differ from occlusion dynamics by a longer duration (warming up is ~15 times longer). Our model is not applicable to its description directly on its entire time domain since the values of h_i/h_e are diverging when we are trying to approximate any highly non-stationary part of the graph (for example, when the blood flow grows with acceleration, which corresponds to the graph sections with $\frac{d^2T}{dt^2} > 0$).

In this case, the blood flow fluctuations can be explained by the central nervous system reaction, since the warming of the nail of the index finger correlates with temperature fluctuations measured on the nails of the remaining fingers that were not subjected to cooling phase (Fig. 5).

We have solved the heat balance Eq. (4) for the case of steady-state blood flow, when $h_i/h_e = \text{const}$, but the solution holds for: (a) local steady-state points, when $\frac{\Delta T_s}{\Delta t} = 0$ and the solution is reduced to the static case (Eq. (7)); (b) weakly non-stationary intervals, when the dynamic solution is approximately correct (Eq. (5)). It follows that we can still use the model if we divide the entire rewarming graph (Fig. 5, dark blue curve) into intervals of rapid change (non-stationary blood flow, the model is not applicable) and stabilization (stationary blood flow, the model is applicable). Some exemplary boundaries of such intervals are highlighted with gray dotted lines in Fig. 5 (see the stat/non-stat captions). The estimates of the blood flow index value carried out in “allowed” points are shown in Fig. 5 in the form of numbers accompanying the graphs. Based on them, one makes a conclusion about a gradual nonlinear increase in blood flow in the index fingernail during its warming (see the graph on the insert of Fig. 4).

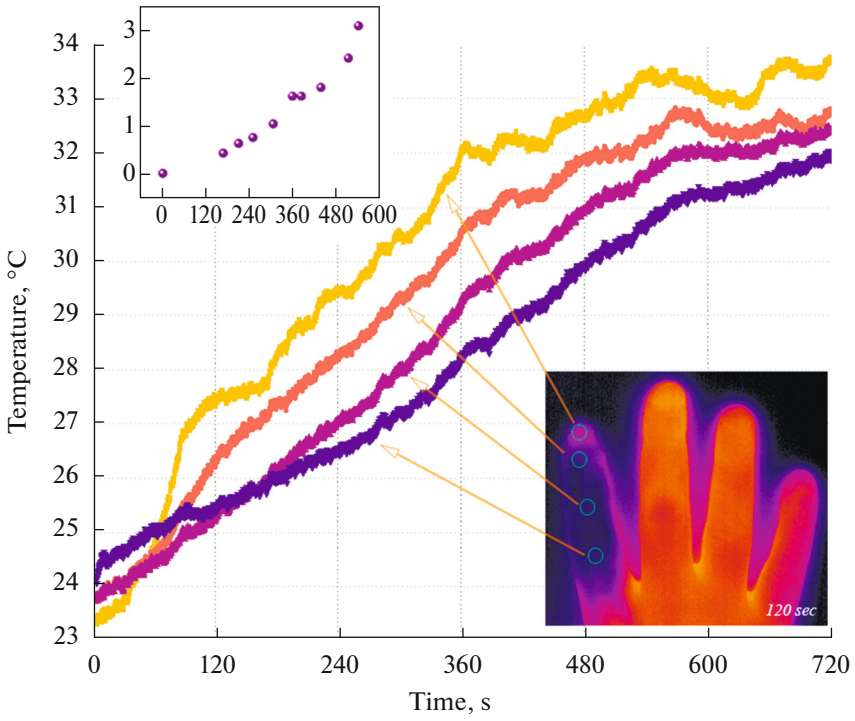

Fig. 4. Rewarming after cooling of different areas of the index finger. The inset on the right shows a thermographic image of the hand corresponding to 120 s of rewarming with the measurement areas indicated. The inset on the left shows a graph of the index h_i/h_e calculated for a certain sampling of points (stationary) of the nail rewarming curve (yellow curve).

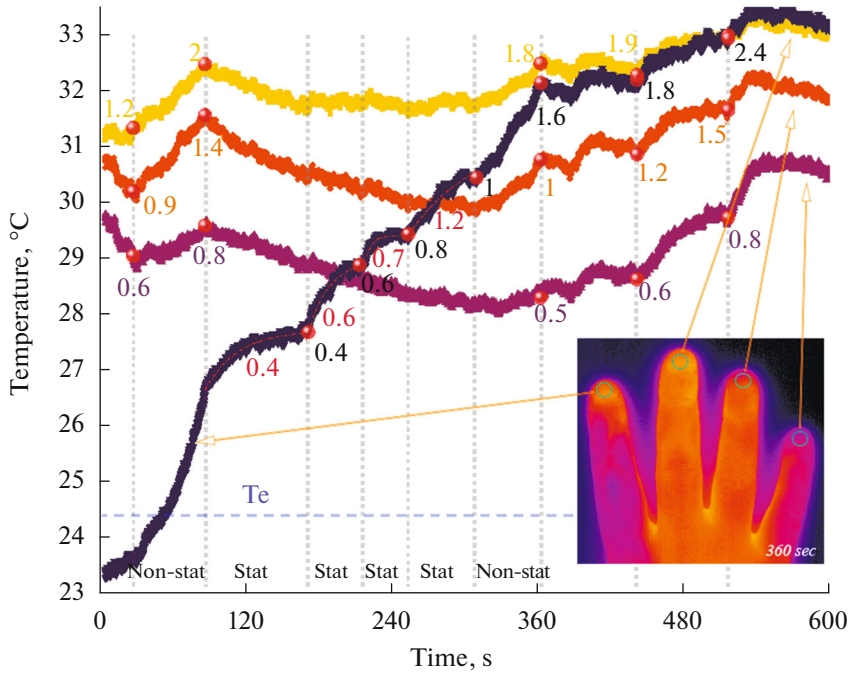

Fig. 5. Temperatures of the nails of four fingers after index finger cooling phase. The temperatures were measured in the areas marked by cyan circles in the thermal image. The next-to-graph numbers show static approximations of the index h_i/h_e calculated for the points marked in red; the red dotted line is a piecewise dynamic approximation of the "allowed" stationary (stat) intervals of stable blood flow. T_e is the room temperature level.

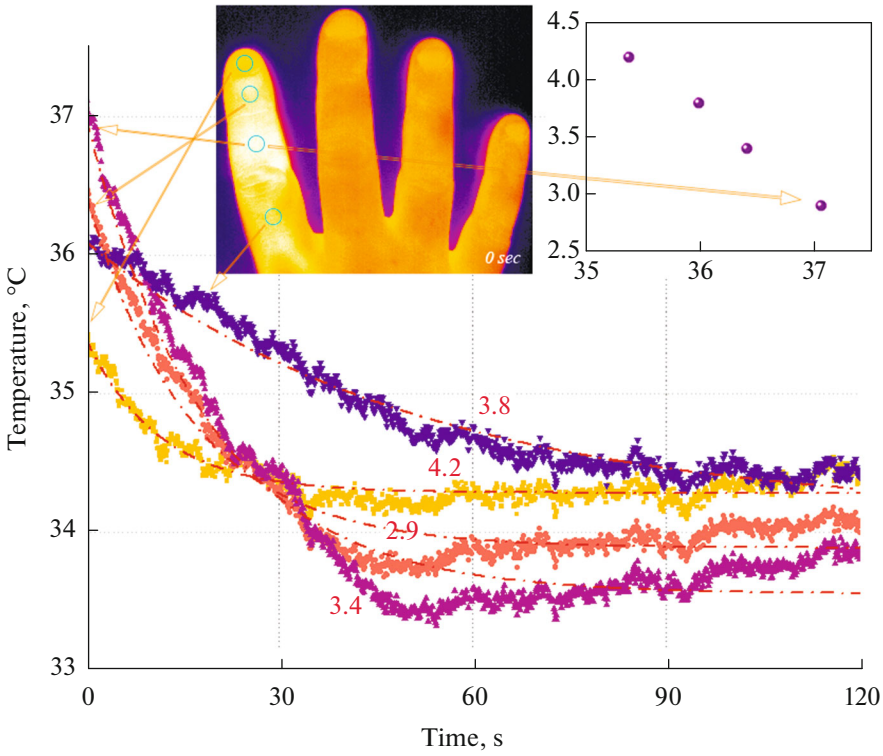

Fig. 6. Cooling the index finger after the heating test. Inserts are thermographic image of the hand corresponding to the onset of cooling; linear dependence between h_i/h_e, calculated from dynamic approximations (red dotted line), and initial heating amplitudes.

The model is also applicable to the assessment of blood flow in local heating dynamic tests. Fig. 6 shows thermometric data corresponding to the recooling of the index finger after immersion in hot water at 60°C for 90 seconds. As can be seen from Fig. 6, the temperature of the finger areas immediately after heating does not exceed 37°C, which indicates effective heat removal by the blood flow throughout the entire heating period. Temperature decreases to normal in just 2 min, which is associated with high blood flow. At the same time, those areas of the finger that demonstrated the lowest blood flow in the normal state and occlusion test (distal and intermediate phalanges in Figs. 2, 3) heat up the most. The linear relationship between the heating amplitude and the blood flow index h_i/h_e is shown in the insert on Fig. 6. It was obtained by applying the model to cooling phase over an entire 2 min interval, i.e. it estimates the average value of the index h_i/h_e over the observation period (estimated numbers are shown in red in Fig. 6). If a more detailed analysis is required, it is possible to establish a division into "allowed" intervals, as in the previous example, but during heating the process of selecting suitable intervals becomes more complicated due to the high background blood flow rate.

Thus, the described heat balance model is applicable for the quantitative description of steady-state blood flow processes that affect the temperature distribution on the skin and is of limited applicability for the analysis of non-stationary processes, which nevertheless can be described if one uses subdivision into "allowed" intervals and points where the model is still valid.

APPLICABILITY LIMITS OF THE HEAT BALANCE MODEL

The temperature begins to fluctuate widely on a timescale up to ten seconds (see the gray frame area in Fig. 2) ~30 s after the occlusion is removed, which is associated with the adaptive multi-level thermoregulatory reaction of the body. Thus, as often happens when working with living objects, the analysis is complicated by the fact that the body through systemic/local reactions can influence the amount of blood flow "from the inside", adjusting it to current needs, and this process can have its own inertia and set of characteristic times. A natural question arises as to whether we are missing any of these important reactions. However, according to extensive experimental data [20, 22] obtained on various warm-blooded animals (including humans), for any individual it is possible to establish a zone of external conditions (the so-called "thermoneutral zone"), in which organism will not use

energy-consuming mechanisms of "emergency response": shivering/pilomotor reflex ("goose-bumps") in the cold, sweating in the heat. In the thermoneutral zone, the main mechanism of thermoregulation (in addition to the behavioral one, i.e., moving to the more comfortable place) will be the mechanism of blood flow regulation, that is, convective heat exchange between deep tissues and the body surface. Such a mechanism turns out to be evolutionarily justified and natural for endothermic animals, since it allows low-effort adaptive adjustment of the heat exchange rate to external conditions. For example, from our data (Fig. 3) it follows that the blood flow in the nail of the index finger can change at least ten-fold. This justifies the introduced interpretation of h_i/h_e as the magnitude of blood flow index under fixed external conditions.

As shown by the rewarming analysis, the highly non-stationary sections corresponding to $h_i/h_e \neq \text{const}$ cannot be analyzed directly using this model, but the model can still be used at locally stationary points where $\frac{\Delta T_s}{\Delta t} = 0$, when the expression for the static temperature T_{static} (7) turns out to hold. In addition, it can be shown that these special points correspond to the extremum points of h_i/h_e index (otherwise there could be no temperature equilibrium, unless h_i and h_e change synchronously, which is unlikely, since h_i depends on the blood flow, while h_e depends on the conditions in the room and on the skin). This allows us to estimate the physiological parameters at stationary points (minima, maxima, and horizontal sections when $T_s(t)$ changes). In general, since the model predicts no inflections in the $T_s(t)$ graph (this can be seen in Fig. 2), the presence of the latter can be interpreted as a deviation from the simple condition $h_i/h_e = \text{const}$, which means constant blood flow level if all other parameters remain fixed. In addition, since Eq. (4) does not contain the $\nabla^2 T$ term, it considers only the part of thermal diffusion (except for the linear part included in the expression for W_i). This is the price of a simplified analysis, and it makes it of limited applicability for situations where the diffusion channel of heat exchange is dominant.

The parameter combination $c\rho L$ in Eq. (5) is generally known only approximately, and although it can be found in a series of observations made under different conditions, this is not necessary, since considered combination h_i/h_e weakly depends on the specific values of cρL from the physiologically acceptable range (although the values of h_i and h_e themselves can change).

Since the surface temperature is the result of the thermal balance between the internal part of the body and the external environment, the analysis is sensitive to external conditions, as with any IR thermometry in general. Only results obtained under similar conditions can be directly compared. The model is one-dimensional, i.e. does not explicitly consider the spatial arrangement of the vessels, and single-layered, i.e. it does not consider the nature of heat transfer between the tissues located between the vessels and the skin surface.

Finally, the model ignores radiative cooling (the nonlinear part), although it is experimentally based on it. This is since the contribution of this heat transfer channel turns out to be negligible for typical external conditions [21].

CONCLUSIONS

It is safe to say that infrared thermometry, which was an expensive and exotic research tool "yesterday", "today" is recognized by the scientific community as promising, and "tomorrow" will become an important part of medical practice helping to save millions of lives. This trend is in part based on non-mentioned implementation of machine learning methods to the data analysis [23–25], in part it can be explained by increased availability of equipment, in part by the simplicity, non-invasiveness and ease of use of the method, and in part by the development of models and methods that allow to extract reliable information about the bioprocesses from temperature distribution patterns. In this paper, we've examined in detail one of the thermal models, using which we've described the results of occlusion, cooling and heating tests of a finger and obtained qualitative and quantitative data on the blood flow rate and circulation in different areas of the finger before and during the tests. The model specificity lies in the fact that it allows for an analytical solution, which eliminates the stage of solving the non-homogeneous differential heat transfer equations numerically yet preserving the main qualitative elements of the heat transfer process. This brings the model to the field of real-time IR thermometry, which is in demand in medical circumstances requiring rapid decision-making, such as intraoperative circulation monitoring.

FUNDING

The work was supported by the research and development project "Informativity of instrumental and laboratory methods for assessing microcirculation during cardiac surgery" (reg. no. FURG-2023-0086).

ETHICS APPROVAL AND CONSENT TO PARTICIPATE

All procedures performed in studies involving human participants were in accordance with the ethical standards of the institutional and/or national research committee and with the 1964 Helsinki Declaration and its later amendments or comparable ethical standards. They were also

approved by the local ethics committee of the Petrovsky National Research Center for Surgery, as documented in Protocol no. 3 dated March 17, 2021.

CONFLICT OF INTEREST

The authors of this work declare that they have no conflicts of interest.

REFERENCES

1. Tansey, E.A. and Johnson, C.D., *Adv. Physiol. Educ.*, 2015, vol. 39, no. 3, p. 139. https://doi.org/10.1152/advan.00126.2014
2. Povolotskiy, A.V., Smirnova, O.S., Soldatova, D.A., and Lukyanov, D.A., *Bull. Russ. Acad. Sci.: Phys.*, 2023, vol. 87, p. 1691. https://doi.org/10.3103/S1062873823703902
3. Neliubov, A.Yu., *Bull. Russ. Acad. Sci.: Phys.*, 2023, vol. 87, p. S421. https://doi.org/10.1134/S1062873823706037
4. Leontyev, A.V., Nurtdinova, L.A., Mityushkin, E.O., Shmelev, A.G., Zharkov, D.K., Andrianov, V.V., Muranova, L.N., Gainutdinov, Kh.L., and Nikiforov, V.G., *Bull. Russ. Acad. Sci.: Phys.*, 2024, vol. 88, p. 853. https://doi.org/10.1134/S1062873824706731
5. Mityushkin, E.O., Shmelev, A.G., Leontyev, A.V., Nurtdinova, L.A., Zharkov, D.K., and Nikiforov, V.G., *Bull. Russ. Acad. Sci.: Phys.*, 2024, vol. 88, no. 12, p. 1993.
6. Bharara, M., Schoess, J., and Armstrong, D.G., *Diabetes/Metab. Res. Rev.*, 2012, vol. 28, no. 1 (suppl.), p. 15. https://doi.org/10.1002/dmrr.2231
7. Kandlikar, S.G., Perez-Raya, I., Raghupathi, P.A., Gonzalez-Hernandez, J.-L., Dabydeen, D., Medeiros, L., and Phatak, P., *Int. J. Heat Mass Transfer*, 2017, vol. 108, p. 2303. https://doi.org/10.1016/j.ijheatmasstransfer.2017.01.086
8. Godoy, S.E., Hayat, M.M., Ramirez, D.A., Myers, S.A., Padilla, R.S., and Krishna, S., *Biomed. Opt. Express*, 2017, vol. 8, no. 4, p. 2301. https://doi.org/10.1364/BOE.8.002301
9. Renkielska, A., Kaczmarek, M., Nowakowski, A., Grudzinski, J., Czapiewski, P., Krajewski, A., and Grobelny, I., *J. Burn Care Res.*, 2014, vol. 35, no. 5, p. 294. https://doi.org/10.1097/BCR.0000000000000059
10. Moreno-Oyervides, A., Diaz-Ojeda, L., Bonilla-Manrique, O.E., Bonastre-Julia, J., Largo-Aramburu, C., Acedo, P., and Martin-Mateos, P., *Sci. Rep.*, 2023, vol. 13, no. 1, p. 16778. https://doi.org/10.1038/s41598-023-44017-6
11. Khan, M.A.B., Hashim, M.J., King, J.K., Govender, R.D., Mustafa, H., and Al Kaabi, J., *J. Epidemiol. Global Health*, 2020, vol. 10, no. 1, p. 107. https://doi.org/10.2991/jegh.k.191028.001
12. Mensah, G.A., Fuster, V., Murray, C.J.L., and Roth, G.A., *J. Am. Coll. Cardiol.*, 2023, vol. 82, no. 25, p. 2350. https://doi.org/10.1016/j.jacc.2023.11.007
13. Sonmez, B., Arbatli, H., Tansal, S., Yagan, N., Unal, M., Demirsoy, E., Tukenmez, F., and Yilmaz, O., *Eur. J. Cardiothorac. Surg.*, 2003, vol. 24, no. 6, p. 961. https://doi.org/10.1016/s1010-7940(03)00519-0
14. Starodubtsev, N.F., Denisenko, V.I., Karimullin, K.R., Kurdoglyan, M.S., Lysenko, S.A., Naumov, A.V., Tagabilev, D.G., and Yuryshev, N.N., *Med. Phys.*, 2023, no. 4, p. 78. https://doi.org/10.52775/1810-200X-2023-100-4-78-83
15. Ince, C., *Crit. Care*, 2015, vol. 19, p. S3. https://doi.org/10.1186/cc14726
16. Guven, G., Hilty, M.P., and Ince, C., *Blood Purif.*, 2020, vol. 49, nos. 1–2, p. 143. https://doi.org/10.1159/000503775
17. De Backer, D., Dubois, M.J., Schmartz, D., Koch, M., Ducart, A., Barvais, L., and Vincent, J.L., *Ann. Thorac. Surg.*, 2009, vol. 88, no. 5, p. 1396. https://doi.org/10.1016/j.athoracsur.2009.07.002
18. Os, M.M., Brom, C.E., van Leeuwen, A.L.I., and Dekker, N.A.M., *Crit. Care*, 2020, vol. 24, no. 1, p. 218. https://doi.org/10.1186/s13054-020-02948-w
19. Roustit, M. and Cracowski, J.L., *Microcirculation*, 2012, vol. 19, no. 1, p. 47. https://doi.org/10.1111/j.1549-8719.2011.00129.x
20. Wright, C.I., Kroner, C.I., and Draijer, R., *J. Pharmacol. Toxicol. Methods*, 2006, vol. 54, no. 1, p. 1. https://doi.org/10.1016/j.vascn.2005.09.004
21. Tattersall, G.J., *Comp. Biochem. Physiol. A: Mol. Integr. Physiol.*, 2016, vol. 202, p. 78. https://doi.org/10.1016/j.cbpa.2016.02.022
22. Johnson, J.M. and Kellogg, D.L., *Front. Biosci.*, 2010, vol. S2, no. 3, p. 825. https://doi.org/10.2741/s105
23. Singh, D. and Singh, A.K., *Comput. Methods Programs Biomed.*, 2020, vol. 183, p. 105074. https://doi.org/10.1016/j.cmpb.2019.105074
24. Stepanov, M.E., Khokhryakova, U.A., Egorova, T.V., Magaryan, K.A., and Naumov, A.V., *Photonics Russ.*, 2024, no. 1, p. 72. https://doi.org/10.22184/1993-7296.FRos.2024.18.1.72.80
25. Stepanov, M.E., Khokhryakova, U.A., Egorova, T.V., Magaryan, K.A., and Naumov, A.V., *Photonics Russ.*, 2024, no. 5, p. 398. https://doi.org/10.22184/1993-7296.FRos.2024.18.5.398.405